Non-Orthogonal Multiple Access with Multi-carrier Index Keying

Eleftherios Chatziantoniou*, Youngwook Ko*, and Jinho Choi†

* School of Electronics, Electrical Engineering and Computer Science, Queen's University Belfast
Belfast, BT7 1NN, United Kingdom
Email: {l.chatziantoniou, y.ko}@qub.ac.uk

†School of Electrical Engineering and Computer Science, Gwangju Institute of Science and Technology (GIST)
Gwangju, 61005, South Korea
Email: jchoi0114@gist.ac.kr

***Abstract*—In this paper a novel transmission scheme that combines non-orthogonal multiple access (NOMA) and multi-carrier index keying (MCIK) is proposed. This scheme is proposed as a mechanism to enable multiple access for dense wireless device-to-device (D2D) systems that require high energy efficiency and effective interference management. The performance of the proposed scheme is analyzed in terms of the pairwise error probability (PEP) of user m. Novel closed-form expressions for the instantaneous and average pairwise error probability (PEP) over Rayleigh fading are derived. These expressions are used to investigate the detection performance of the proposed scheme over different configurations. Furthermore, a closed-form expression that approximates the overall average PEP is derived. This expression enables the performance analysis of NOMA-MCIK within acceptable accuracy levels. The performance of the proposed scheme is assessed through numerical and simulation results.**

***Index Terms*—Device-to-device (D2D), multi-carrier index keying (MCIK), non-orthogonal multiple access (NOMA), orthogonal frequency division multiplexing (OFDM), pairwise error probability (PEP).**

I. Introduction

Non-orthogonal multiple access (NOMA) has been recently proposed as a multiple access technique to enhance the spectrum efficiency of future radio access networks [1]. Different from previous generations of wireless systems such as 3GPP LTE, which were based on the time, frequency, and code domain, NOMA uses the power domain to allow multiple access. Therefore, in NOMA schemes, multiple users can share both time and frequency resources, while multiple access is possible by properly adjusting the power allocation. The key idea behind NOMA is to superimpose messages for multiple users in the power domain and then use successive interference cancellation (SIC) for efficient detection. In particular, users with better channel conditions remove the signals indented for other users by applying SIC and decode their own signals. NOMA has also been considered to improve the cell-edge throughput and achieve low latency. As a result, NOMA is envisioned as potential candidate for efficient wireless connectivity of billions of devices, as a practical realisation of the Internet of Things (IoT) concept.

An uplink NOMA scheme, which enables more than one user to share the same sub-carrier without any coding or spreading redundancy, has been proposed in [2]. The performance of NOMA with randomly deployed users was considered in [3], whereas NOMA was introduced in a cognitive radio network in [4]. Furthermore, a multiple-input multiple-output (MIMO) NOMA system was proposed in [5].

Multi-carrier index keying (MCIK) is a new multi-carrier technique, which has been recently proposed as a means of extending the conventional two dimensional M-ary signal constellations to a third dimension, which is the sub-carrier index [6]. In every MCIK-OFDM transmission only a subset of sub-carriers is activated, according to the incoming data, to convey constellation symbols. The use of the sub-carrier indices as an additional degree of freedom enables the transmission of extra information bits without any additional bandwidth and power requirements.

As a result, MCIK-OFDM constitutes a promising modulation technique for providing high data-rate services especially for low-cost, energy constrained wireless systems such as device-to-device (D2D) communications. MCIK-OFDM has attracted significant attention as it can provide a balanced trade-off between error performance and spectral efficiency [7]. To this end, different MCIK-OFDM transceiver architectures have been proposed and analyzed over different fading conditions including [8], [9].

In this paper a multi-carrier NOMA scheme termed as NOMA-MCIK is proposed. This scheme combines NOMA with MCIK to superimpose MCIK blocks of multiple users in the power domain. This approach can benefit from the advantages of both NOMA and MCIK. By activating different sub-carriers for each user NOMA-MCIK can be used as a means of limiting interference in dense D2D deployments. Furthermore, by using multiple sub-carriers to transmit the same signal for users with limited channel conditions can increase the diversity gain of the systems and improve the performance at the cell edge. As a result, NOMA-MCIK can be used to provide reliable multiple access for wireless D2D systems. To this end, novel closed-form expressions for the instantaneous and average PEP are derived. Using the moment generating function (MGF) approach, a generalized

framework for the error performance of NOMA-MCIK users is introduced, which facilitates the performance analysis of the proposed scheme for various fading distributions. Furthermore, the derived expressions account for any number of active sub-carriers, which in turn, enables the performance analysis of different NOMA-MCIK concepts by investigating the effects of interference and power allocation ratios to the PEP performance.

The remainder of the paper is organised as follows. The system model of the proposed hybrid NOMA-MCIK scheme is introduced in Section II. In Section III novel closed-form expressions for the exact instantaneous and average overall PEP for NOMA-MCIK with maximum likelihood detection are derived. A tight approximation for the average PEP over Rayleigh fading is also derived. In Section IV numerical and simulation results are presented. Section V draws the conclusion of this work.

II. NOMA-MCIK System Model

Consider a downlink (DL) NOMA system with a single transmitter (TX) and M users uniformly distributed. Without loss of generality, a single antenna scenario is considered with h_m denoting the channel between TX and the user m. In classical NOMA, at each transmission, TX transmits $\sum_{m=1}^{M}\sqrt{\alpha_m P}s_m$, where s_m is the signal of user m, P is the transmission power and α_m is the corresponding power allocation coefficient with $\alpha_1 \geq ... \geq \alpha_M$ and $\sum_{i=1}^{M}\alpha_m = 1$. Throughout this paper a scenario with only two users is considered, as shown in Fig. 1.

The received signal at user m is given as

$$y_m = h_m s + n_m,\ m = 1, 2, \tag{1}$$

where $s = (\sqrt{\alpha_1 P}s_1 + \sqrt{\alpha_2 P}s_2)$ and n_m denotes the background noise at user m modelled as additive white Gaussian noise (AWGN) i.e., $n_m \sim \mathcal{CN}(0, N_0)$.

Different from classical NOMA systems, in NOMA-MCIK each user employs MCIK to create its signal block, $\mathbf{s}_m$ using L_m orthogonal sub-carriers with $\kappa_1, ..., \kappa_{L_m}$ denoting the index of each sub-carrier, which are grouped into β_m blocks of z_m sub-carriers such that $\beta_m = L_m/z_m$. The number of active sub-blocks of user m is denoted by N_m. Each MCIK block is superimposed in the power domain by scaling the total transmit power by an appropriate power allocation coefficient for each user, as shown in Fig. 2.

At each NOMA-MCIK transmission $K_m = N_m \times z_m$ out of L_m sub-carriers are activated to convey K_m copies of data symbol s. For each user, the number and the index of the active-sub-carriers may vary. More specifically, for given N_m active sub-blocks let $\mathbf{I}_m = \{i_1, ..., i_{K_m}\}$, where $i_k \in [1, ..., L_m]$ for $k = 1, ...K_m$, denote the indices of the active sub-carriers of user m. The corresponding signal of user m is denoted by $\mathbf{s_m} = [s(1), ..., s(L_m)]^T$, where $s(l) = s$ for $I \in \mathbf{I}_m$ and $s(j) = 0$ for $j \notin \mathbf{I}_m$.

One of the main aspects of NOMA-MCIK is the transmission of the same signal through multiple sub-carriers, which can increase the diversity gain of the system. More specifically, it is proposed that by increasing the number of active sub-carriers based on the distance between TX and user m, the performance at the cell edge will be improved. Indicatively, the further the user from TX the more sub-carriers are activated to increase its diversity order as means of improving its vulnerability to interference. In addition, the activation of different number of sub-carriers for each user is expected to limit the interference by reducing the likelihood of the active sub-carriers of different users to interfere with each other. Therefore, NOMA-MCIK constitutes a promising solution that enables reliable transmission for user m.

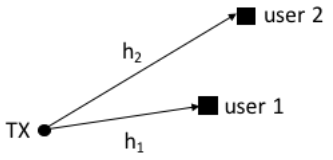

Fig. 1. NOMA scheme with two users.

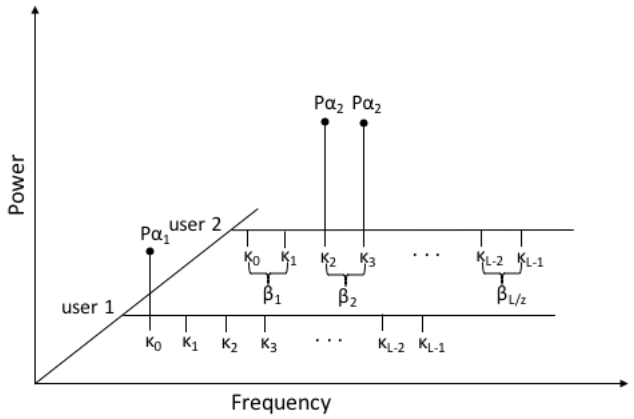

Fig. 2. NOMA-MCIK block for two users with $L_1 = L_2 = L$ total sub-carriers, $N_1 = N_2 = 1$ active sub-blocks and different block sizes $z_1 = 1$, $z_2 = 2$.

Using MCIK-based NOMA across the L_m sub-carriers in the frequency domain, let the channel matrix from TX to users 1 and 2 be denoted by $\mathbf{H}_1$ and $\mathbf{H}_2$, respectively. The received signals at users 1 and 2 are obtained as

$$\tilde{\mathbf{y}}_1 = \mathbf{H}_1(\sqrt{\alpha_1 P}\mathbf{s}_1 + \sqrt{\alpha_2 P}\mathbf{s}_2) + \mathbf{n}_1 \tag{2}$$

$$\mathbf{y}_2 = \mathbf{H}_2(\sqrt{\alpha_1 P}\mathbf{s}_1 + \sqrt{\alpha_2 P}\mathbf{s}_2) + \mathbf{n}_2, \tag{3}$$

where $\mathbf{s}_1$ and $\mathbf{s}_2$ denote the MCIK signal block of users 1 and 2 respectively, $\mathbf{H}_1 = diag(h_1(1), ..., h_1(L_1))$, $\mathbf{H}_2 = diag(h_2(1), ..., h_2(L_2))$ where $h_m(I)$ represents the channel fading coefficient of sub-carrier l at user m, and $\mathbf{n}_1$, $\mathbf{n}_2$ are AWGN vectors, i.e., $\mathbf{n}_m \sim \mathcal{CN}(\mathbf{0}, N_0\mathbf{I})$, for $m \in \{1, 2\}$.

Let user 1 be placed closer to TX than user 2. As a result, the channel gain of user 1 is higher than user 2. By using SIC user 1 can detect $\mathbf{s}_1$ by detecting and removing $\mathbf{s}_2$ from its observation, while user 2 detects $\mathbf{s}_2$ treating $\mathbf{s}_1$ as noise. Therefore, after SIC (2) can be rewritten as

$$\mathbf{y}_1 = \mathbf{H}_1\sqrt{\alpha_1 P}\mathbf{s}_1 + \mathbf{n}_1. \tag{4}$$

Accordingly, for NOMA-MCIK, the receiver has to detect the indices of the active sub-carriers (or, equivalently, the index

of active sub-block). Therefore, by applying the well known maximum likelihood (ML) detector to estimate the indices of the active sub-carriers, the detection process for $\mathbf{s}_1$ and $\mathbf{s}_2$ can be mathematically described as

$$\hat{\boldsymbol{s}}_1 = \arg\min_{\mathbf{s}_1} ||\mathbf{y}_1 - \mathbf{H}_1\sqrt{\alpha_1 P}\mathbf{s}_1||^2 \tag{5}$$

$$\hat{\boldsymbol{s}}_2 = \arg\min_{\mathbf{s}_2} ||\mathbf{y}_2 - \mathbf{H}_2\sqrt{\alpha_1 P}\mathbf{s}_2||^2. \tag{6}$$

Note that for $\mathbf{s}_1$ the detection process is similar to classical MCIK because $\mathbf{s}_2$ can be effectively detected and removed by SIC. On the other hand, it is clear that the detection of $\mathbf{s}_2$ is affected by the signal of user 1.

III. Performance Analysis

In order to gain an insight into the performance of the proposed scheme, the detection error of the active sub-carriers within the NOMA-MCIK sub-blocks is considered. In this context, consider the pairwise error event (PEE) that an active sub-block index κ is incorrectly detected as the index of an inactive sub-block $\tilde{\kappa}$ for κ, $\tilde{\kappa} \in \{1, ..., \beta_m\}$ and $\kappa \neq \tilde{\kappa}$. Then the PEP can be defined as the probability of the PEE to occur, i.e., P($\kappa \to \tilde{\kappa}$). To this end, the performance of NOMA-MCIK is analyzed in terms of both the instantaneous and average PEP.

A. Instantaneous PEP

1) User 1: By applying ML detection to $\mathbf{y}_1$, as described in (5), the conditional PEP of user 1 is obtained as [10]

$$P^1(\kappa \to \tilde{\kappa}) = Q\left(\frac{1}{2}\sqrt{\frac{\alpha_1 P||\mathbf{h}_1(\kappa) - \mathbf{h}_1(\tilde{\kappa})||^2}{N_0}}\right), \tag{7}$$

where $\mathbf{h}_1(\kappa)$ and $\mathbf{h}_1(\tilde{\kappa})$ denote channel vectors of active sub-block and inactive sub-block, respectively, with $\|\mathbf{h}_1(\kappa)\|_0 = K_1$, $\mathbf{h}_1(\cdot)$ denoting a zero vector except non-zero elements at sub-carriers of sub-block κ and $\tilde{\kappa}$, respectively, and $Q(x) = 1/\sqrt{2\pi}\int_x^\infty e^{-t^2/2}dt$ is the error function.

Using the law of the total probability and the union bound, the upper bound on the overall PEP is derived as,

$$P_e^1 \leq \sum_{\kappa=1}^{L_1/K_1} \sum_{\tilde{\kappa}\neq\kappa=1}^{L/K_1-N_1} Q\left(\sqrt{\frac{\alpha_1 P||\mathbf{h}_1(\kappa) - \mathbf{h}_1(\tilde{\kappa})||^2}{4N_0}}\right)\rho, \tag{8}$$

where $\rho = \frac{N_1}{L_1/K_1}$.

2) User 2: Similarly, by applying ML detection at user 2 as described in (6) the instantaneous PEP can be obtained as

$$P^2(\kappa \to \tilde{\kappa}) = Q\left(\frac{1}{2}\sqrt{\frac{\alpha_2 P||\mathbf{h}_2(\kappa) - \mathbf{h}_2(\tilde{\kappa})||^2}{L_1 N_0 + \alpha_1 P x_{21}}}\right), \tag{9}$$

where $\mathbf{h}_2(\kappa)$ and $\mathbf{h}_2(\tilde{\kappa})$ denote the channel vectors of active sub-block and inactive sub-block, respectively, with $\|\mathbf{h}_2(\kappa)\|_0 = K_2$, $\|\mathbf{h}_2(\tilde{\kappa})\|_0 = K_2$, and x_{21} denotes the power of sub-channel whose index relies on $\mathbf{s}_1$. From (9) it can be seen that the PEP of user 2 is now based on the signal to interference plus noise ratio (SINR). More specifically, $L_1 N_0$ and $\alpha_1 P x_{21}$ correspond to the power of the noise of L sub-carriers and interference due to the signal of user 1.

By following the same approach an upper bound on the overall PEP for user 2 is obtained as

$$P_e^2 \leq \sum_{\kappa=1}^{L_2/K_2} \sum_{\tilde{\kappa}\neq\kappa=1}^{L_2/K_2-N_2} Q\left(\frac{1}{2}\sqrt{\frac{\alpha_2 P||\mathbf{h}_2(\kappa) - \mathbf{h}_2(\tilde{\kappa})||^2}{L_1 N_0 + \alpha_1 P x_{21}}}\right)\rho, \tag{10}$$

where $\rho = \frac{N_2}{L_1/K_2}$.

B. Average PEP over Rayleigh fading

1) User 1: At user 1 the average PEP over Rayleigh is the same as in MCIK-OFDM, which has been derived in [11]. Hence, the overall average PEP for user 1 is obtained as

$$\begin{aligned}\bar{P}_e^1 &\leq \sum_{\kappa=1}^{L_1/K_1} \sum_{\tilde{\kappa}\neq\kappa=1}^{L_1/K_1-N_1} \left(1 + \frac{\alpha_1\bar{\gamma}}{8}\right)^{-2K_1} \rho \\ &= N_1 \frac{L_1/K_1 - N_1}{2}\left(1 + \frac{\alpha_1\bar{\gamma}}{8}\right)^{-2K_1},\end{aligned} \tag{11}$$

where $\bar{\gamma}$ denotes the average signal-to-noise ratio (SNR).

2) User 2: By using the improved Chernoff bound for the Q-function, i.e., $Q(x) = 0.5\exp(-x^2/2)$ and some mathematical manipulation (10) can be rewritten as

$$P_e^2 \leq \sum_{\kappa=1}^{L_2/K_2} \sum_{\tilde{\kappa}\neq\kappa=1}^{L_2/K_2-N_2} \exp\left(-\frac{1}{8}\frac{\alpha_2 P x_2}{L_1 N_0 + \alpha_1 P x_{21}}\right)\frac{\rho}{2}, \tag{12}$$

where $x_{21} \sim \chi^2_{4K_1}$ and $x_2 \sim \chi^2_{4K_2}$ are chi-squared distributed random variables.

The average PEP can be obtained by first taking the expectation of (12) as

$$\begin{aligned}\bar{P}_e^2 &\leq \sum_{\kappa=1}^{L_2/K_2} \sum_{\tilde{\kappa}\neq\kappa=1}^{L_2/K_2-N_2} \mathbb{E}_{x_2,x_{21}}\left\{\exp\left(-\frac{1}{8}\frac{\alpha_2 P x_2}{L_1 N_0 + \alpha_1 P x_{21}}\right)\right\}\frac{\rho}{2} \\ &= \sum_{\kappa=1}^{L_2/K_2} \sum_{\tilde{\kappa}\neq\kappa=1}^{L_2/K_2-N_2} \underbrace{\mathbb{E}_{x_2}\left\{\mathbb{E}_{x_{21}}\left\{\exp\left(-\frac{1}{8}\frac{\alpha_2 P x_2}{L_1 N_0 + \alpha_1 P x_{21}}\right)\right\}\right\}}_{\mathrm{z}}\frac{\rho}{2}.\end{aligned} \tag{13}$$

Assuming that x_{21} and x_2 are independent and using Jensens' inequality, i.e., $\mathbb{E}\{f(.)\} \leq f(\mathbb{E}(.))$, term Z of (13) can be rewritten as

$$\begin{aligned}Z &\leq \mathbb{E}_{x_2}\left\{\exp\left(-\frac{1}{8}\frac{\alpha_2 P x_2}{L N_0 + \alpha_1 P \mathbb{E} x_{21}}\right)\right\} \\ &= \mathbb{E}_{x_2}\left\{\exp\left(-\frac{1}{8}\frac{\alpha_2 P x_2}{L_1 N_0 + \alpha_1 P \sigma^2}\right)\right\} \\ &= \mathbb{M}_{x_2}\left\{-\frac{1}{8}\frac{\alpha_2 P \sigma^2}{L_1 N_0 + \alpha_1 P \sigma^2}\right\},\end{aligned} \tag{14}$$

where $\mathbb{M}_x(t)$ represents the MGF of random variable x and σ^2 denotes the variance of the sub-carrier channel.

Assuming that x_2 is modelled as a chi-squared distribution with $4K_2$ degrees of freedom its corresponding MGF is given as

$$\mathbb{M} = (1 - t)^{-2K_2}. \tag{15}$$

Hence, by substituting (15) into (13) for $t = -\frac{1}{8}\frac{\alpha_2 P\sigma^2}{L_1 N_0+\alpha_1 P\sigma^2}$, and after some mathematical manipulations, an upper bound on the overall average PEP of NOMA-MCIK over Rayleigh fading is derived as

$$\begin{aligned}\bar{P}_e^2 &\leq \sum_{\kappa=1}^{L_2/K_2}\sum_{\tilde{\kappa}\neq\kappa=1}^{L_2/K_2-N_2}\left(1+\frac{1}{8}\frac{\alpha_2\bar{\gamma}}{L_1+\alpha_1\bar{\gamma}}\right)^{-2K_2}\frac{\rho}{2}\\ &= N_2\frac{L_2/K_2-N_2}{2}\left(1+\frac{1}{8}\frac{\alpha_2\bar{\gamma}}{L_1+\alpha_1\bar{\gamma}}\right)^{-2K_2},\end{aligned} \tag{16}$$

where $\bar{\gamma}$ denotes the average SNR of the system.

From (16) it can be seen that the average PEP can be improved by increasing the diversity order of the system. This can be achieved by increasing the number of active sub-carriers whose indices convey the information.

C. Improved Approximation of Average PEP

From (11) and (16) it can be seen that the average PEP of users 1 and 2 is obtained as an upper bound. A tight approximation for the average PEP can be obtained by using the approximation $Q(x) \simeq \frac{1}{12}e^{-x^2/2}+\frac{1}{4}e^{-2x^2/3}$ which has been found to approximate the Q-function more accurately than the improved Chernoff bound [12].

Therefore, by following the same approach as in the previous subsection an approximation for the average PEP over Rayleigh fading for user 1 is derived as

$$\begin{aligned}\bar{P}^1_{e_{approx}} \simeq N_1\left(\frac{L_1}{K_1}-N_1\right)\Bigg[&\frac{1}{12}\left(1+\frac{\alpha_1\bar{\gamma}}{8}\right)^{-2K_1}\\ &+\frac{1}{4}\left(1+\frac{\alpha_1\bar{\gamma}}{6}\right)^{-2K_1}\Bigg].\end{aligned} \tag{17}$$

Similarly, a tight approximation for the average PEP over Rayleigh fading for user 2 can be obtained as

$$\begin{aligned}\bar{P}^2_{e_{approx}} \simeq N_2\left(\frac{L_2}{K_2}-N_2\right)\Bigg[&\frac{1}{12}\left(1+\frac{1}{8}\frac{\alpha_2\bar{\gamma}}{L_1+\alpha_1\bar{\gamma}}\right)^{-2K_2}\\ &+\frac{1}{4}\left(1+\frac{1}{6}\frac{\alpha_2\bar{\gamma}}{L_1+\alpha_1\bar{\gamma}}\right)^{-2K_2}\Bigg].\end{aligned} \tag{18}$$

IV. Numerical Results and Discussion

In this section numerical and simulation results are presented for a NOMA-MCIK scheme with two users over Rayleigh fading. For simplicity on the analysis it is assumed that $L_1 = L_2 = L$ and $z_1 = 1, z_2 = 2$. Therefore, the transmission for user 1 is configured with $L = 8$, $K_1 = 1$ and $N_1 = 1$ whereas for user 2 two different configurations are considered: 1) $L = 8$, $K_2 = 2$ and $N_2 = 1$ and 2) $L = 8$, $K_2 = 4$ and $N_2 = 1$. For each scenario three different power allocation schemes are taken into account: 1) $\alpha_1 = 0.4$ $\alpha_2 = 0.6$; 2) $\alpha_1 = 0.2$ $\alpha_2 = 0.8$ and 3) $\alpha_1 = 0.01$ $\alpha_2 = 0.99$.

Fig. 3 depicts the average PEP performance for users 1 and 2 with the first configuration and different power allocation coefficients. It is shown that the detection performance is significantly affected by the power allocation coefficient and the SNR. More specifically, it can be observed that user 2 achieves better error performance than user 1 at low SNR regions. This can also be verified from (17) which results in diversity order $d = 4$ for $K_2 = 2$. Interestingly, an error floor at user 2 has been observed at high SNR regions. As the SNR of both users increases, the effect of interference from user 1 becomes dominant, which in turn results to an error floor at approximately $E_s/N_0 = 25$ dB for the two first power allocation schemes. On the other hand, the error performance of user 2 can significantly be improved with negligible error floor when higher power is allocated to user 2 compared to user 1. Furthermore, the closeness between the simulation and numerical results from (17) and (18) validates the derivation and reveals the tightness of the derived expressions for the average PEP of users 1 and 2 especially for high SNR regions.

Fig. 4 compares the performance of user 2 in terms of the average PEP for different configurations and power allocation strategies. It is shown that the error performance of user 2 can be improved by increasing the number of active sub-carriers per sub-block especially for the cases when $\alpha_2 = 0.6$ and $\alpha_2 = 0.8$. Therefore, for the case of high interference from user 1, the performance of user 2 can be improved by increasing the number of active sub-carriers within a given sub-block.

In all previous cases, it is assumed that user 1 and user 2 have the same SNR statistics. However, it is worth investigating the case when the SNR of user 1 increases at different rates over the SNR of user 2. In this context, let $\bar{\gamma}$ denote the SNR of user 2, whereas the SNR of user 1 is given as $\bar{\gamma}\tau$, with $\tau \geq 1$, where τ expresses the rate of change in the SNR. In this context, Fig. 5 depicts the average PEP of users 1 and 2 for the case when the SNR of user 1 increases at different rate, $\tau = \{3, 5, 10\}$ dB over the SNR of user 2 for a power allocation with $\{\alpha_1, \alpha_2\} = \{0.01, 0.99\}$. It is observed that the average PEP performance of user 2 degrades when the SNR of user 1 increases resulting on higher error floor. On the other hand, the performance of user 1 improves with a 7 dB power gain as τ increases from 3 dB to 10 dB for an average PEP of $10^{-}4$.

V. Conclusion

In this paper novel NOMA scheme with index modulation has been proposed. Novel closed-form expressions for the instantaneous and average overall PEP for NOMA-MCIK with ML detection are derived. These expression are used to analyze the performance of user m for a NOMA-MCIK scheme in the presence of interference. Furthermore, a closed-form expression that approximated the overall average PEP has been derived. The approximate expression achieves acceptable accuracy levels of less than 1 dB, at high SNR regions. The derived expressions enable the performance analysis for various concepts of NOMA-MCIK. Particularly, combining MCIK with NOMA allows both power and sub-carrier index dimensions to be properly used and decrease the error performance faster with high diversity order obtained. Interestingly, the error floor at user 2 was observed to depend on the interference of user 1,

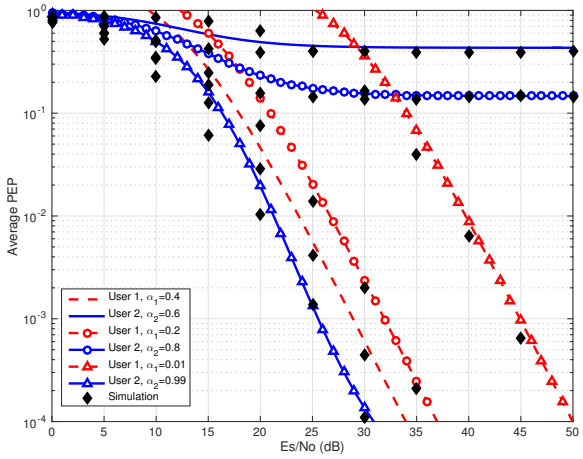

Fig. 3. Average PEP performance comparison between user 1 and user 2 for $L = 8$ with $\{K_1, N_1\} = \{1, 1\}$ and $\{K_2, N_2\} = \{2, 1\}$ and three different power allocation strategies.

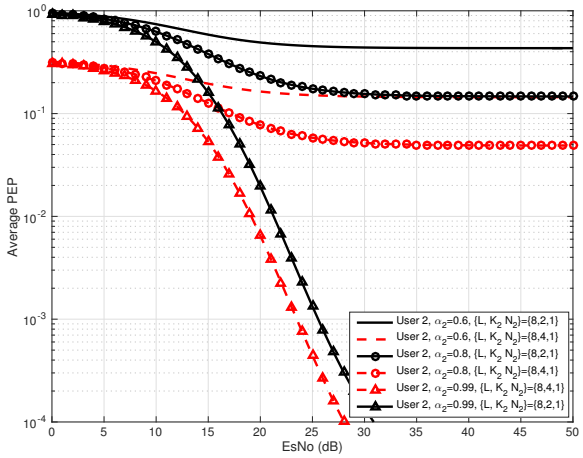

Fig. 4. Average PEP performance for user 2 with different configuration and power allocation strategies.

which can be significantly reduced by the use of joint power allocation and sub-carrier index activation. Future work will focus on applying different detection techniques, extending the analysis to account for outage probability and optimise the NOMA-MCIK to improve the overall performance in terms of spectral efficiency.

ACKNOWLEDGMENT

This work has been supported by the Engineering and Physical Sciences Research Council (EPSRC) grant with reference number EP-M015521-1.

REFERENCES

[1] J. Choi, "Non-Orthogonal Multiple Access in Downlink Coordinated Two-Point Systems," *IEEE Commun. Lett.*, pp.313-316, Feb. 2014.

[2] M. Al-Imari, P. Xiao, M. A. Imran, and R. Tafazolli, "Uplink non-orthogonal multiple access for 5G wireless networks," *in Proc. of Intern. Symposium on Wireless Commun. Systems,* pp. 781-785, Aug. 2014.

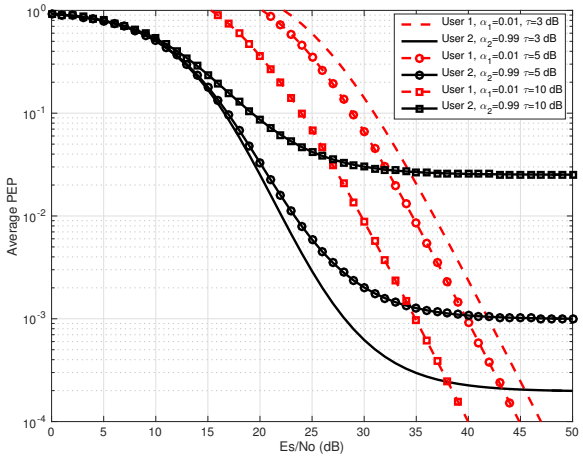

Fig. 5. Average PEP over Rayleigh fading for user 2 with user 1 SNR increasing at different rates, i.e, $\tau = 3, 5, 10$ dB for $L = 8$ and $\{K_2, N_2\} = \{2, 1\}$ and $\{\alpha_1, \alpha_2\} = \{0.01, 0.99\}$.

[3] Z. Ding, Z. Yang, P. Fan and H. V. Poor, " On the performance of non-orthogonal multiple access in 5G systems with randomly deployed users," *IEEE Signal Process. Lett*, , vol. 21, no. 12, pp. 1501-1505, Dec. 2014.

[4] Y. Liu, Z. Ding, M. Elkashlan, and J. Yuan,"Non-orthogonal multiple access in large-scale underlay cognitive radio networks," *IEEE Trans. Veh. Technol.*, vol. PP, no. 99, pp. 1-1, 2016

[5] Z. Ding, F. Adachi, and H. Poor, "The application of MIMO to non-orthogonal multiple access," *IEEE Trans. Wireless Commun.,* vol. 15,no. 1, pp. 537?552, Jan. 2016.

[6] R. Abu-alhiga, and H. Haas, "Subcarrier-index modulation OFDM," *in Proc. IEEE Pers., Indoor, Mobile Radio Commun.*, pp.177-171 Sep. 2009.

[7] E. Basar, U. Aygolu, E. Panayirci, and H. Poor, "Orthogonal frequency division multiplexing with index modulation," *IEEE Trans. Signal Process.*, vol. 61, pp. 5536-5549, Nov. 2013.

[8] E. Chatziantoniou, J. Crawford and Y. Ko "Performance analysis of a low complexity detector for MCIK-OFDM over TWDP fading," *IEEE Commun. Lett*, vol. 20, no. 6, pp. 1251-1254, Jun. 2016.

[9] E. Chatziantoniou, J. Crawford and Y. Ko "A Low Complexity Detector with MRC Diversity Reception for MCIK-OFDM," *in Proc. IEEE Pers., Indoor, Mobile Radio Commun.*, pp.1071-1074 Sep. 2016.

[10] Y. Ko, "A tight upper bound on bit error rate of joint OFDM and multicarrier index keying,"*IEEE Commun. Lett.* vol. 18, pp. 1763-1766, Oct. 2014.

[11] Y. Ko, "Selective multi-carrier index keying OFDM: Error propagation rate with moment generating function," *in IEEE Proc. Int. Workshop on Signal Process. Adv. in Wireless Commun.*, pp. 1-6, Jul. 2016.

[12] M. Chiani, D. Dardari and M. K. Simon, "New exponential bounds and approximations for the computation of error probability in fading channels," *IEEE Trans. on Wireless Commun.,* vol. 2, no. 4, pp. 840-845, Jul. 2003.